

PLA and PBAT-Based Electrospun Fibers Functionalized with Antibacterial Bio-Based Polymers

A. Chiloeches, R. Fernández-García, M. Fernández-García, A. Mariano, I. Bigioni, A. Scotto d'Abusco,* C. Echeverría,* and A. Muñoz-Bonilla*

Antimicrobial fibers based on biodegradable polymers, poly(lactic acid) (PLA), and poly(butylene adipate-co-terephthalate) (PBAT) are prepared by electrospinning. For this purpose, a biodegradable/bio-based polyitaconate containing azoles groups (PTTI) is incorporated at 10 wt.% into the electrospinning formulations. The resulting fibers functionalized with azole moieties are uniform and free of beads. Then, the accessible azole groups are subjected to *N*-alkylation, treatment that provides cationic azolium groups with antibacterial activity at the surface of fibers. The positive charge density, roughness, and wettability of the cationic fibers are evaluated and compared with flat films. It is confirmed that these parameters exert an important effect on the antimicrobial properties, as well as the length of the alkylating agent and the hydrophobicity of the matrix. The quaternized PLA/PTTI fibers exhibit the highest efficiency against the tested bacteria, yielding a 4-Log reduction against *S. aureus* and 1.7-Log against MRSA. Then, biocompatibility and bioactivity of the fibers are evaluated in terms of adhesion, morphology and viability of fibroblasts. The results show no cytotoxic effect of the samples, however, a cytostatic effect is appreciated, which is ascribed to the strong electrostatic interactions between the positive charge at the fiber surface and the negative charge of the cell membranes.

products.^[1-3] Electrospinning is a very versatile technique that fabricates fiber with nano- to micrometer range diameters and controlled surface morphology, leading mats with unique characteristics: i) high specific surface area, ii) porous structure, which allows desired permeability and exudation, and iii) structure similar to an extracellular matrix that favors the cell attachment and proliferation. Besides, electrospinning allows the incorporation of additional functionalities into fibers, such as bioactive components, growth factors, or antimicrobial compounds that would improve the performance of these materials in biomedical applications such as wound dressing uses. In fact, wound infection is one of the major risk factors for wound healing failure, and complications in chronic wounds. Also, microbial contamination of implants, vessels, meshes of other devices provokes devastating infections, sepsis and often requires prompt removal of the devices. The incorporation of antimicrobial agents into biomaterials could help to combat these problems.^[4-9] In the design of

1. Introduction

Polymeric fibers produced by electrospinning have been extensively studied in the past years for biomedical applications such as artificial vessels, scaffolds, and fibrous wound dressings and matrices because they present several advantages over traditional

such products for clinical applications, biodegradable and biocompatible polymers, including polylactic acid (PLA), polycaprolactone (PCL), poly(glycolic acid) (PGA), or poly(butylene adipate-co-terephthalate) (PBAT), are gaining increased importance as they metabolize in human body into biocompatible degradation products, and second surgery for removal is unnecessary.^[10,11]


A. Chiloeches, M. Fernández-García, C. Echeverría, A. Muñoz-Bonilla
 Instituto de Ciencia y Tecnología de Polímeros (ICTP-CSIC)
 C/ Juan de la Cierva 3, Madrid 28006, Spain
 E-mail: cecheverria@ictp.csic.es; sbonilla@ictp.csic.es

A. Chiloeches
 Escuela Internacional de Doctorado de la Universidad Nacional de Educación a Distancia (UNED)
 C/ Bravo Murillo, 38, Madrid 28015, Spain

R. Fernández-García
 Hospital Universitario de Móstoles C/ Dr. Luis Montes
 s/n, Móstoles, Madrid 28935, Spain

M. Fernández-García, C. Echeverría, A. Muñoz-Bonilla
 Interdisciplinary Platform for Sustainable Plastics towards a Circular Economy-Spanish National Research Council (SusPlast-CSIC)
 Madrid Spain

A. Mariano, I. Bigioni, A. Scotto d'Abusco
 Department of Biochemical Sciences
 Sapienza University of Rome
 P.le A. Moro, 5, Rome 00185, Italy
 E-mail: anna.scottodabusco@uniroma1.it

 The ORCID identification number(s) for the author(s) of this article can be found under <https://doi.org/10.1002/mabi.202200401>

© 2022 The Authors. Macromolecular Bioscience published by Wiley-VCH GmbH. This is an open access article under the terms of the Creative Commons Attribution License, which permits use, distribution and reproduction in any medium, provided the original work is properly cited.

DOI: 10.1002/mabi.202200401

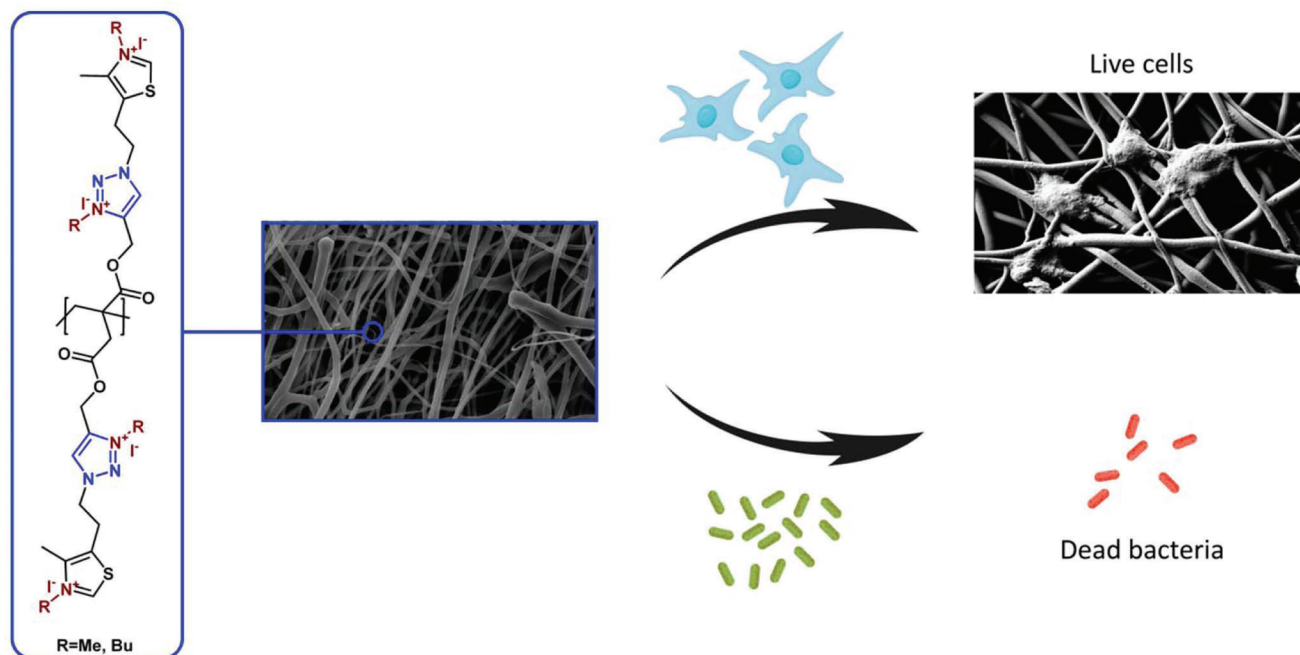


Figure 1. Schematic representation of functionalized polymeric fibers with PTTI-Me and PTTI-Bu derivatives and their interactions with cells and bacteria.

Among all, PLA is one of the most widely used biopolymers due to its processing properties, full biodegradability, biocompatibility, and because it is approved for clinical use.^[12] Although PLA has favorable mechanical properties, neat PLA exhibits brittleness with poor impact. PBAT, a biodegradable aliphatic–aromatic copolyester, is more flexible and has high elongation at break; however, has low tensile modulus. Both polymers have been also blended together to develop materials with enhanced mechanical properties.^[13,14] PBAT, as PLA, is biocompatible but has been scarcely studied as a biomaterial for medical applications. Anyhow, PLA and PBAT have hydrophobic nature, lack of cell recognition signals, and their cell adhesion, proliferation and differentiation properties are poor.^[12,15–17] Incorporation of bioactive compounds, such as hydroxyapatite, heparin and hyaluronic acid, inside the polymer matrix or at the surface of the materials are a promising strategy to improve hydrophilicity and biocompatibility.^[18,19] However, other bioactive compounds, such as antimicrobial agents, could compromise the biocompatibility and biodegradability. Traditionally, quaternary ammonium salts, phosphonium salts, metal ions, and antibiotics are employed to impart antimicrobial activity to materials;^[20–22] however, their use is normally accompanied by residual toxicity or a rapid increase in bacterial resistance. Antimicrobial polymers offer some important advantages, such as thermal and chemical stability, long-term activity, and lower level of bacterial resistance.^[23,24] Nevertheless, most of the reported antimicrobial polymers are derived from petroleum-sources, which jeopardize the biodegradability of the final material and might also affect the biocompatibility.

In this work, an antibacterial bio-based and biodegradable polymer derived from itaconic acid was employed to impart antibacterial character to PLA and PBAT fiber mats obtained by electrospinning. In addition, for comparative purpose, this antibacterial polymer was incorporated into flat PBAT-based films

prepared by melt-extrusion and compression molding. Then, we studied the interactions between these functionalized materials with bacteria and eukaryotic fibroblast cells to determine their antimicrobial efficacy, bioactivity and safety for biomedical applications.

2. Results and Discussion

2.1. Preparation of Antimicrobial Electrospun Fibers Based on PLA/PTTI and PBAT/PTTI

The bio-based antimicrobial polymers, poly(bis((1-(2-(4-methylthiazol-5-yl)ethyl)-1H-1,2,3-triazol-4-yl)methyl) itaconate) quaternized with methyl and butyl iodide, PTTI-Me and PTTI-Bu, respectively, previously developed by our group were initially employed to impart antibacterial activity to PLA and PBAT electrospun fibers (**Figure 1**).

However, the antibacterial polymers PTTI-Me and PTTI-Bu containing cationic groups were not soluble in the solvent mixture compatible with PLA and PBAT employed in the electrospinning process. Therefore, to avoid heterogeneity and aggregation problems, we used the antibacterial precursor PTTI polymer, which is neutrally charged and soluble in the electrospinning solution. Thus, this polymer was incorporated into the CHCl_3/DMF (9:1) solvent mixture at 10 wt.% together with 90 wt.% of PLA or PBAT, at a total polymer concentration of 20 wt.%. Subsequently, from these solutions, PLA or PBAT-based fibers loaded with the PTTI polymer bearing triazole groups were successfully obtained by electrospinning. Likewise, PLA and PBAT fibers were also prepared under similar conditions and used for comparison purpose. **Figure 2** displays scanning electron microscopy (SEM) images of all prepared fibers. We can appreciate that the incorporation of the PTTI polymer reduces

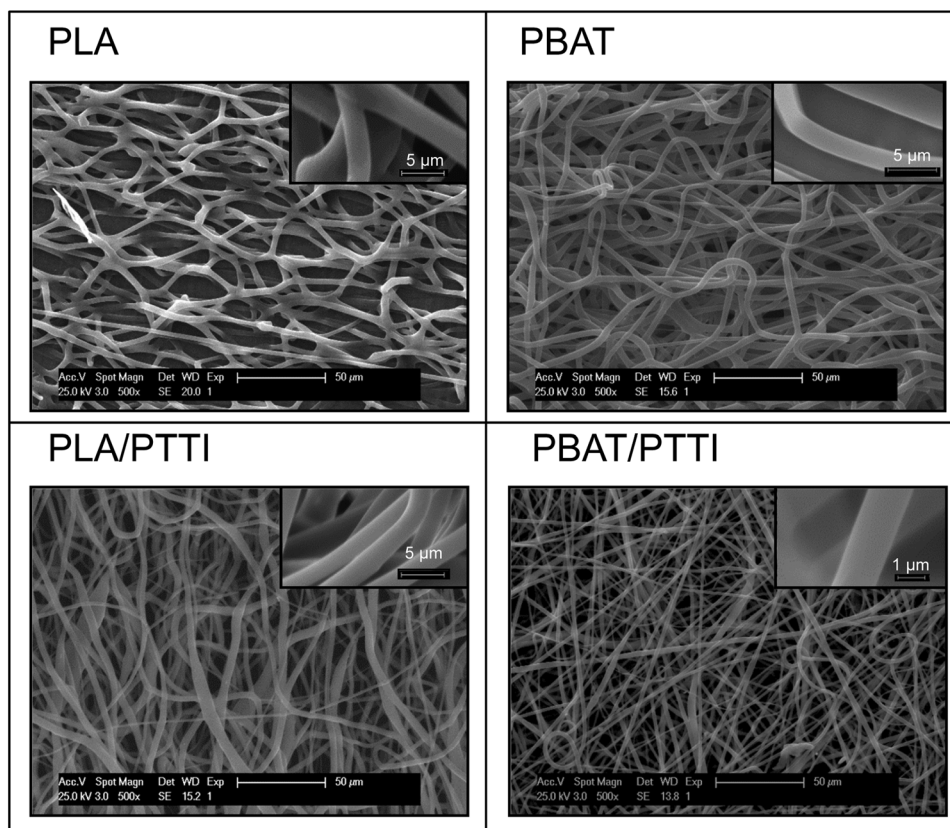


Figure 2. SEM images of PLA, PBAT, PLA/PTTI, and PBAT/PTTI electrospun fibers.

the diameter of the obtained fibers in both cases, PLA and PBAT-based fibers. While the average diameter of electrospun PLA fibers was $4 \pm 1 \mu\text{m}$, the PLA/PTTI fibers present a value of $3.5 \pm 1.2 \mu\text{m}$. Similarly, the average diameter diminishes from $3 \pm 1 \mu\text{m}$ for PBAT fibers to $2.1 \pm 0.6 \mu\text{m}$ for PBAT/PTTI fibers. The addition of this cationic polymer into the electrospinning solutions may modify characteristics such as viscosity, density, conductivity solution, and factors that affect the final fiber diameter.^[25] Although the homogeneity is somehow reduced with the incorporation of the PTTI polymers, bead-free and uniform fibers with smooth surfaces were obtained (see insets of figures for higher magnification images).

Fourier transform infrared (FTIR) spectroscopy was employed to confirm that the polymers did not undergo any degradation during the electrospinning process. FTIR spectra displayed in Figure S1 (Supporting Information) show that PLA and PBAT-based fibers exhibit the band characteristics of such polymers without any evidence of degradation. PLA/PTTI and PBAT/PTTI have almost identical spectra, and new bands associated to PTTI polymers were not visible due to the low content of this polymer and overlapping of the signal. To confirm the presence of PTTI in the fibers, extractions with DMSO- d_6 were performed and analyzed by ^1H -nuclear magnetic resonance (NMR) spectroscopy. Figure S2 (Supporting Information) shows the ^1H -NMR spectrum of PTTI polymer and the signal assignment, demonstrating the stability of the polymer throughout the electrospinning process.

The PBAT and PLA-based fibers loaded with PTTI polymer precursor were subsequently surface functionalized to provide antimicrobial activity. *N*-alkylation reaction of the triazole and thiazole groups available at the surface was carried out with iodomethane or iodobutane to afford the corresponding cationic azolium groups (PLA/PTTI-Me, PLA/PTTI-Bu, PBAT/PTTI-Me, and PBAT/PTTI-Bu). These positively charged chains are responsible of the antimicrobial character as they can interact with the negatively charged membrane causing cell leakage and eventually bacterial death.^[26,27] The success of the quaternization reaction at the surface of the fibers was confirmed by ^1H -NMR spectroscopy of the quaternized PTTI extracted in DMSO- d_6 (Figure S2, Supporting information), in which the peaks associated to azolium groups (≈ 10.08 and ≈ 9.20 ppm) can be observed. Positive charge density of the surface has a large influence on the killing efficiency charge densities of greater than $1\text{--}5 \times 10^{15}$ are typically needed for a good activity^[28,29]; therefore, these positive charges were quantified by measuring the accessible cationic units able to selectively bind anionic fluorescein molecules. The fluorescein adsorbed on the surface was subsequently desorbed with cetyltrimethylammonium bromide (CTAB) and quantified by UV-vis spectroscopy. Table 1 summarizes the charge density obtained at the surface of PLA and PBAT-based fibers after *N*-alkylation reaction with two different alkylating agents. The estimated charge density at the surface of fibers was found to be $\approx 10^{14}\text{--}10^{15} \text{ N}^+ \text{ cm}^{-2}$, values near to other contact-active antibacterial surfaces.^[30] Remarkably, the fibers quaternized

Table 1. Antibacterial activity expressed as percentage of bacterial reduction (%) and Log reduction (Log) of tested fibers and films against, *Staphylococcus aureus* (*S. aureus*), Methicillin resistant *Staphylococcus aureus* (MRSA), and *Pseudomonas aeruginosa* (*P. aeruginosa*). Surface charge of tested fibers and films expressed as $N^+ \text{ cm}^{-2}$.

	<i>S. aureus</i>		MRSA		<i>P. aeruginosa</i>		Surface charge [$N^+ \text{ cm}^{-2}$]
	[%]	Log	[%]	Log	[%]	Log	
PLA/PTTI-Me	99.99	4	98.1	1.7	38	0.2	6×10^{15}
PLA/PTTI-Bu	41.0	0.26	–	–	–	–	4×10^{14}
PBAT/PTTI-Me	82.9	0.76	99.93	3.2	–	–	3×10^{15}
PBAT/PTTI-Bu	69.6	0.52	92.8	1.1	–	–	3×10^{14}
FilmPBAT/PTTI-Me	92.3	1.11	74.8	0.6	50	0.3	9×10^{14}
FilmPBAT/PTTI-Bu	99.7	2.46	99.4	2.2	58	0.4	8×10^{14}

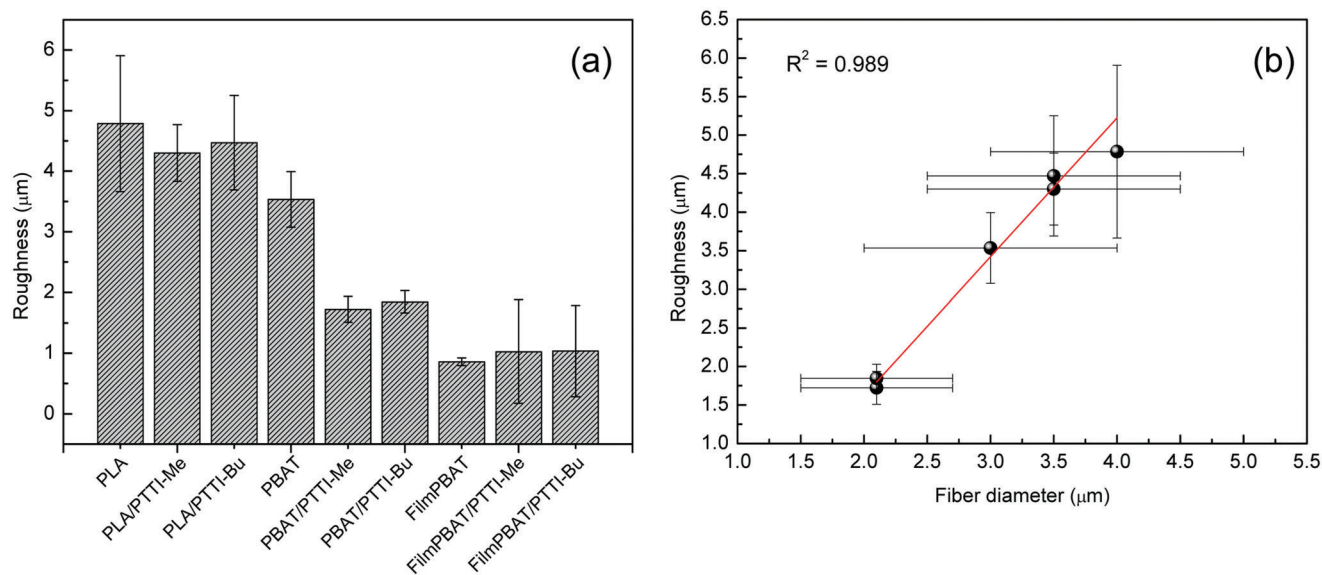


Figure 3. a) Roughness R_a of the obtained fiber mats and films and b) roughness values compared to the fiber diameter (the red line is a linear trend line with corresponding R^2 value).

with iodomethane exhibit values higher than $10^{15} N^+ \text{ cm}^{-2}$, thus, sufficient charge to disrupt the bacterial cell wall and hence high antibacterial activity. It is clearly appreciated that charge density lowered drastically when the quaternization reaction was performed with iodobutane, which is consistent with the general trend observed that the degree of quaternization decreases with increasing size of the alkylating agent due to steric effect.^[31]

The roughness of the obtained fiber mats was also measured as a key parameter influencing the bioactivity of the material surface. **Figure 3** displays the surface roughness, R_a , of the mats and its correlation with the fiber diameter.

The roughness of the fiber mats loaded with the polyitaconate antimicrobial polymers (PTTI-Me and PTTI-Bu) is lower than that of neat PLA and PBAT fibers. As previously reported and clearly observed in **Figure 3b**, the surface roughness measured in electrospun fibers was found to augment with the diameter of the constituent fibers.^[32] As expected, no differences were found between methylated and butylated samples, because the fibers were subjected to surface modification by N-alkylation reaction

in a post-electrospinning reaction, and the fiber diameter did not vary. Surface roughness also plays an important role in the wettability of a surface, which will affect the contact and interactions between surface and biological environment.^[33] Then, water contact angles were measured to assess the surface wettability of the obtained fiber mats and films. **Figure 4** collects the obtained contact angle values for all the tested materials. It is clearly seen that electrospun fibers exhibited very high water contact angles due to the surface roughness, as previously reported.^[34,35] Slight differences in the contact angle values can be observed between PLA- and PBAT-based fibers due to the smaller diameters found for PBAT-based fibers and also due to the higher hydrophobicity of PBAT in comparison with PLA. The decrease in the fiber diameters causes an increase in contact angle because the topography influences air entrapment between the fiber interfaces and hence modifies the liquid–solid interface.^[34] As expected, PBAT films with smooth surfaces exhibit much lower contact angle values than fiber mats. However, the differences found between functionalized surfaces with polyitaconate derivatives and

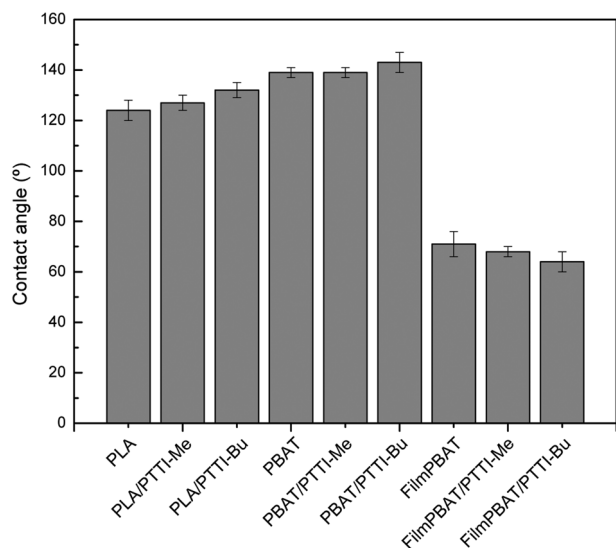


Figure 4. Contact angle measurements of the obtained fiber mats and films.

non-functionalized samples were not significant, suggesting that the predominant factors affecting wettability are the topography and surface roughness as observed in other studies.^[35]

2.2. Preparation of Antimicrobial Films Based on PBAT/PTTI

Subsequently, biodegradable antimicrobial films were prepared through the incorporation of the polyitaconate derivatives into the biopolymers, by melt extrusion followed by compression molding. However, these polyitaconate derivatives exhibit moderate thermal resistance with degradation temperatures below 200 °C.^[36] For this reason, these antimicrobial polymers can be only used in processing treatments up to ≈ 150 °C. Accordingly in this work, PTTI-Me and PTTI-Bu antimicrobial polymers were only incorporated in PBAT films, a biodegradable polymer of low processing temperature, whereas PLA films could not perform due to its processing temperature ≈ 200 °C. Thus, PTTI-Me and PTTI-Bu (10 wt.%) were directly extruded together with PBAT pellets and then films were obtained via compression molding. The films obtained were labeled as FilmPBAT/PTTI-Me and FilmPBAT/PTTI-Bu. The FTIR spectra of the resulting films confirmed that the polymers did not suffer any appreciable degradation process during extrusion and compression molding (see Figure S3, Supporting Information). Subsequently, the number of cationic groups accessible at the surface of the films, which are responsible of the antimicrobial character, was estimated from the titration method using fluorescein as described above. In this case, similar charge density was obtained from films functionalized with methylated PTTI-Me and butylated PTTI-Bu, 9×10^{14} and 8×10^{14} N⁺ cm⁻², respectively, because the polyitaconate were previously and almost completely quaternized before the blend extrusion process with PBAT. Remarkably, in these films containing the cationic polymers with high number of positive charge, the surface charge is much lower than that obtained in the PLA/PTTI-Me fibers, in which, in principle, only the thiazole and triazole groups available at the surface were quaternized.

This can be explained by the large surface area of the fiber mats in comparison with the films. Besides and as expected, the roughness of these films is much lower than the value obtained for the fibers (see Figure 3).

2.3. Antibacterial Efficacy

In previous works, our group has demonstrated the antimicrobial effectivity of the cationic polymers PTTI-Me and PTTI-Bu against Gram-positive bacteria.^[37] Besides, the polymer quaternized with butyl iodide showed higher inhibitory activity because longer hydrophobic alkyl chains provides stronger antibacterial activity as generally improves the insertion into and disruption of the bacterial membrane, which is in agreement with previous reports.^[38] In this work, the antibacterial activity of PLA and PBAT-based fiber mats and PBAT films loaded with 10 wt.% of PTTI-Me and PTTI-Bu was evaluated against Gram-positive, *S. aureus* and *Methicillin-Resistant S. aureus* and Gram-negative, *P. aeruginosa* bacteria. In the antibacterial test, fiber mats and films of 1 × 1 cm² were inoculated in 10 mL of bacterial suspension (10⁵ CFUs mL⁻¹). Controls of PLA and PBAT fibers and PBAT film alone, and an inoculum without fibers were also tested. After 24 h of incubation, the percentage of bacterial viable count reduction related to controls upon contact with antibacterial fibers and films were determined and summarized in Table 1.

The results clearly indicate, as expected, that all tested samples are more effective against Gram-positive bacteria, *S. aureus*, and MRSA. It was also appreciated a correlation between surface charge and antibacterial activity. In fiber mats, the samples quaternized with iodobutane, PLA/PTTI-Bu, and PBAT/PTTI-Bu, exhibit significantly much less activity, with lower bacterial reduction, than the fibers quaternized with iodomethane, which present higher number of positive charge at their surface, with values above 1×10^{15} N⁺ cm⁻². As proposed before, the *N*-alkylation reaction with long chain lengths provokes a significant drop in conversion, and then, in the surface charge due to steric effect. It has to be mentioned that butylated and methylated fibers had similar roughness values, then, this factor would not contribute to this difference found in the antibacterial activity. Remarkably, the PLA/PTTI-Me fibers yield a 4-Log reduction after 24 h of contact against *S. aureus*, 1.7-Log reduction against MRSA, and 0.21 against *P. aeruginosa*. When comparing PLA and PBAT-based fibers, PLA based fibers with higher surface charge and also higher roughness were found to kill significantly more bacteria than the corresponding PBAT-based fibers. This can be attributed to the higher hydrophobicity thus, lower water wettability of PBAT, which could affect the *N*-alkylation reaction and also to the contact between bacteria and surface material.

Concerning the results of the PBAT-based films, in contrast to the fiber mats, the sample contained the butylated polymer (FilmPBAT/PTTI-Bu) exhibits higher antibacterial activity than the methylated polymer (FilmPBAT/PTTI-Me) against all tested microorganisms. This finding can be explained on the basis of the similar surface charge density achieved in both mats, in which the difference between them lies in the length of the alkylating chain. In this case, almost completely quaternized polymers, with similar number of cationic groups, were incorporated directly to the PBAT matrix, then; the length of the

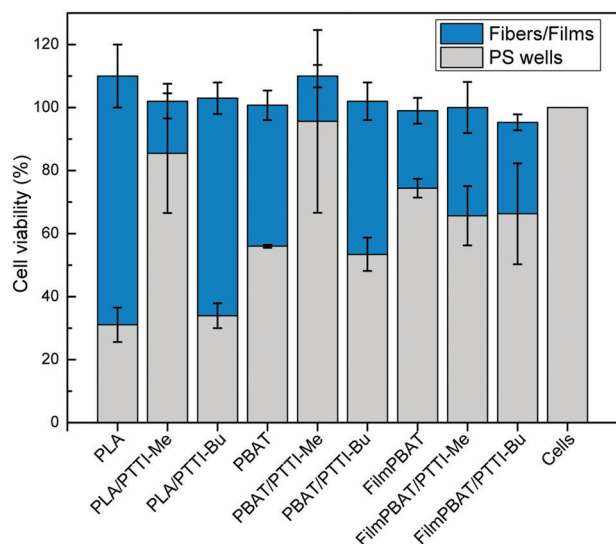


Figure 5. Cell viability of fibroblast seeded onto tested fibers and films assessed by MTS assay using cells seeded in well cell culture plate as negative control 100% viability. Cells adsorbed into the material surfaces are represented in blue, cells remained into cell culture plate are represented in gray. Results are expressed as mean \pm SEM of data obtained by three independent experiments.

hydrophobic alkylating chain (butyl or methyl) is the key factor affecting the antimicrobial activity. The hydrophilic/hydrophobic character is crucial in the design of antimicrobial polymeric materials, as cationic charge may bind to the bacterial membrane through electrostatic attraction while hydrophobic part is needed to insert into the inner hydrophobic core of the membrane.^[39]

2.4. Cells Viability and Cells Grow on Fibers and Films Surfaces

Subsequently, we analyzed the biocompatibility and bioactivity of the antimicrobial fibers and films, in terms of adhesion, morphology and viability of fibroblasts. Fibroblasts viability onto these fiber mats and films based on PLA and PBAT was assessed by MTS-based colorimetric assay at 24 h. We analyzed both, the cells adhered onto the samples and the cells not adhered and remained in the bottom of the wells. **Figure 5** shows the cell viability of cells adsorbed and cells remained into cell culture plate in comparison with cells seeded in 96-well cell culture plates considered as negative control (100% viability). The sum of both measurements shows that the antimicrobial fiber mats and films are not toxic against human fibroblasts and not detrimental for cell viability, with a viability percentage close to 100%

When focusing on the cells adsorbed onto the surface of PBAT and PLA-based samples, several parameters, such as roughness, hydrophilicity, surface charge, and influence cell–material interaction. **Figure 5** clearly shows that PLA fibers are able to attach more fibroblasts (absorbance of 3-(4,5-dimethylthiazol-2-yl)-5-(3-carboxymethoxyphenyl)-2-(4-sulfophenyl)-2H-tetrazolium, MTS) than PBAT fibers, because the higher hydrophobicity of PBAT would suppress the adhesion of fibroblasts, thereby inhibiting their growth.

Roughness of PBAT-based fibers is also lower than that found for PLA fibers, which also could have a negative effect on the cell

adhesion. This effect is even more evident in FilmPBAT sample, with lower roughness. Another interesting finding is the effect of the surface charge density on cell growth. When PLA/PTTI-Me and PLA/PTTI-Bu fibers, with similar R_a values, were compared, a significant difference in cell adhesion is appreciated, which can be associated to the surface charge. This variation in cells adhered on the surface depending on the butylated and methylated sample is not manifested in the prepared films, probably because the surface charge is almost similar. In principle, the incorporation of cationic groups at the surface of biomaterials can enhance cell adhesion and growth due to electrostatic interactions with the negatively charged cell membrane.^[40,41] However, in methylated PLA/PTTI-Me samples with high positive charge density, $6 \times 10^{15} \text{ N}^+ \text{ cm}^{-2}$, the cell adhesion is considerably reduced; showing the best results in the PLA/PTTI-Bu fibers. Similar behavior was obtained for PBAT-based fibers, in which PBAT/PTTI-Bu fiber mat seems to be a more suitable platform for fibroblasts adhesion and proliferation than the methylated sample. It was suggested previously that extremely high interaction between fibroblasts and surface material would alter the cell growth and have a cytostatic effect.^[18] Thus, although moderate positive surface charge could have a positive effect on cell adhesion because increases hydrophilicity, high charge density can inhibit cell proliferation.

Next, morphology of the cells seeded on these fiber mats was studied by SEM (**Figure 6**). Fibroblasts seeded on PLA and PBAT fibers showed a flattened and thin morphology and good spread after 24 h of incubation. However, fibroblasts present more spherical shape when adhered to fibers containing PTTI-Me and PTTI-Bu antimicrobial polymers, indicating limited cell spreading and cell constriction. This rounded and irregular morphology is more evident in the samples with PTTI-Me samples, containing higher number of positive surface charges.

These results seem to indicate, in effect, a cytostatic effect of these positive-charged PLA- and PBAT-based materials on human fibroblast cells, which is associated to the strong adhesion of the cells on the surface, reducing the spreading capability and affecting the growth and viability. Cytostatic effect has been observed previously in cationic functionalized surfaces with chitosan^[18] and polyethylenimine.^[42] Cells adhere rapidly and strongly to such surfaces and sequester the adhesion molecules in the early steps of cell-surface interaction. This cytostatic property observed in the obtained fiber mats opens the possibility of application in anti-adhesion treatments to reduce, for instance, peritoneal adhesion, which causes numerous complications in postsurgery processes.^[43]

3. Conclusion

In summary, biodegradable PLA and PBAT homogeneous fibers with antibacterial properties were developed incorporating a bio-based polytaconate derivative with thiazole and triazole groups into the electrospinning process. These azole functional groups accessible at the surface of fibers were subjected to *N*-alkylation with either butyl or methyl iodide leading cationic fibers. Lower surface charge density was obtained in butylated fibers in comparison with methylated surfaces due to steric hindrance. The roughness also influences the surface charge of the prepared materials, when we compared electrospun fibers and flat films

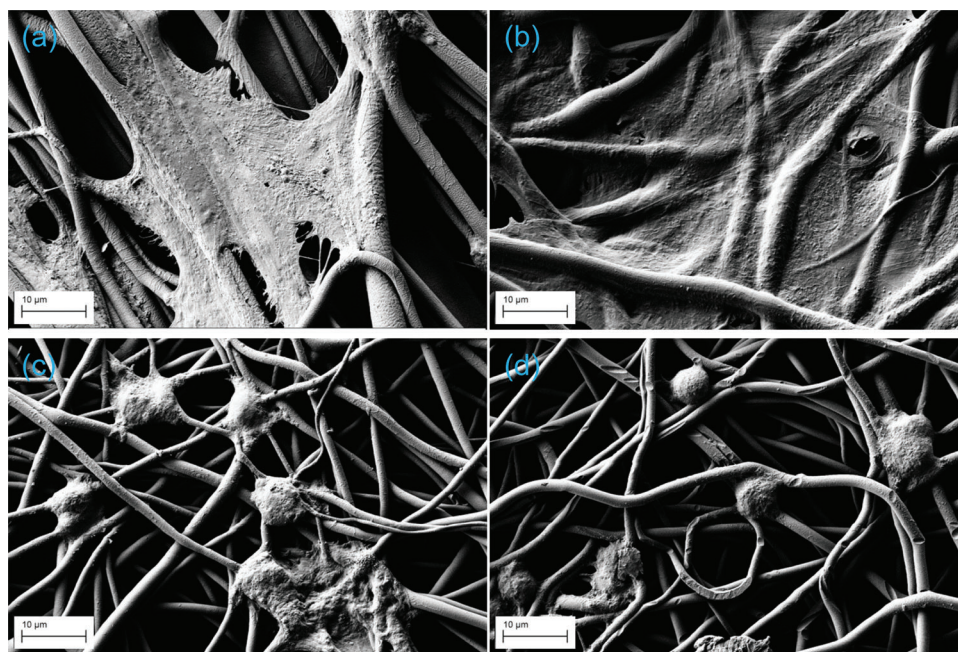


Figure 6. SEM images of Human dermal primary fibroblasts growth for 24 h on a) PLA fiber mat, b) PBAT fiber mat, c) PBAT/PTTI-Bu fiber mat, and d) PBAT/PTTI-Me fiber mat.

obtained by compression molding. This surface charge density had a direct correlation with the antibacterial activity, the highest the positive charge density the highest the activity. However, when we compared films with similar charge density, those quaternized with iodobutane exhibit better efficiency as long alkylating chains improve hydrophobic/hydrophilic balance, key factor for antimicrobial activity. Although the prepared materials exhibit significant antibacterial activity against Gram-positive bacteria, and non-toxicity against human fibroblast, the morphological analysis of the cells seeded on the surface of cationic fibers showed a cytostatic effect, with potential in anti-adhesion post-surgery treatments.

4. Experimental Section

Materials: Fluorescein sodium salt and cetyltrimethylammonium bromide (CTAB, $\geq 98\%$) were purchased from Merck and used as received. 3-(4,5-Dimethylthiazol-2-yl)-5-(3-carboxymethoxyphenyl)-2-(4-sulfophenyl)-2H-tetrazolium (MTS) was obtained from Promega Corporation. All the organic solvents were of AR grade. *N,N*-dimethylformamide (DMF) and chloroform (CHCl_3) were obtained from Scharlau. Polylactic acid (PLA, 6202D) was obtained from Natureworks while Ecoflex (PBAT) was provided by BASF. The precursor antibacterial polymer synthesized from itaconic acid, poly(bis((1-(2-(4-methylthiazol-5-yl)ethyl)-1H-1,2,3-triazol-4-yl)methyl) itaconate) (PTTI), and the corresponding cationic polymers obtained after *N*-alkylation reaction with methyl and butyl iodide (PTTI-Me or PTTI-Bu), were synthesized according to the procedure previously described.^[37]

For the antibacterial assay phosphate buffered saline powder (pH 7.4) and sodium chloride solution (NaCl suitable for cell culture, BioXtra) were purchased from Sigma-Aldrich. The 96 well microplates were acquired from BD Biosciences. Columbia agar (5% sheep blood) plates were obtained from Fisher Scientific. For American Type Culture Collection (ATCC), *Pseudomonas aeruginosa* (*P. aeruginosa*, ATCC 27 853), *Staphylococcus aureus* (*S. aureus*, ATCC 29 213), and *Staphylococcus aureus* resistant

to methicillin and oxacillin (MRSA, ATCC 43 300) were used as bacterial strains and purchased from Oxoid.

Electrospinning Process: Electrospinning solutions were prepared by dissolving the polymeric blends (PLA/PTTI or PBAT/PTTI) in a 90/10 v/v mixture of CHCl_3 /DMF at a concentration of 20%w/w. The polymer ratio was 90% of PLA or PBAT and 10% of PTTI in weight. PLA and PBAT blank solutions were also prepared. From these solutions, electrospun polymeric fibers were obtained using a homemade electrospinner with horizontal configuration equipped with a syringe needle connected to a high voltage power. The fiber mats were collected at room temperature and at 30% of relative humidity, in a grounded aluminum foil collector located perpendicular at 12 cm from the needle tip, at flow rate of 1 mL h^{-1} and by applying a voltage at 16 kV for 30 min. The obtained PLA/PTTI, PBAT/PTTI, PLA, and PBAT fiber mats were dried under vacuum at room temperature for 24 h to remove any residual solvent.

Preparation of the Antimicrobial Fiber Mats, *N*-Alkylation of the Fibers: PLA/PTTI and PBAT/PTTI fibers mats were subjected to *N*-alkylation of the triazol and thiazol groups available at the surface to obtain antimicrobial functional fibers containing cationic triazolium and thiazolium groups. Briefly, PLA/PTTI and PBAT/PTTI electrospun mats were cut into squares of $1 \times 1 \text{ cm}$, and each of these substrates were immersed in 1 mL of methanol solution containing a large excess of methyl iodide or butyl iodide (200 μL). After 10 days of incubation at 37 °C for *N*-alkylation reaction, the mats were rinsed several times with methanol to remove any residual reagents to afford PLA/PTTI-Me, PLA/PTTI-Bu, PBAT/PTTI-Me, and PBAT/PTTI-Bu antimicrobial fibers.

Preparation of the Antimicrobial Films of PBAT: Antimicrobial films were prepared by melt-extrusion in a microextruder equipped with twin conical co-rotating screws (MiniLab Haake Rheomex CTW5, Thermo Scientific) with a capacity of 7 cm^3 . PBAT pellets (90 wt.%) and antimicrobial polymers (10 wt.%) (PTTI-Me or PTTI-Bu) were blended and processed at temperature of 140 °C in the microextruder using a screw rotation rate of 100 rpm, and a residence time of 5 min. Likewise, PBAT pellets were also melt-extruded using similar conditions.

Each extruded sample was subsequently processed into films by compression molding at 140 °C in a hot press (Dr. COLLIN 200 \times 200) using a film mold (50 \times 50 mm^2). The samples were kept between the plates at atmospheric pressure for 2 min until melting and they were further

submitted to the following pressure cycle, 20 kPa for 1 min, 50 kPa for 1 min, and finally the obtained films were quenched to room temperature at 10 kPa for 2 min. The resulting film formulations were labeled as FilmP-BAT, FilmPBAT/PTTI-Me, and FilmPBAT/PTTI-Bu.

Characterization: Fourier transform infrared (FTIR) spectra of the fibers were recorded on a Perkin Elmer Spectrum Two instrument equipped with an attenuated total reflection (ATR) module. ¹H NMR spectra were recorded on a Bruker Avance III HD-400AVIII spectrometer at room temperature using DMSO-d₆ purchased from Sigma–Aldrich as solvent.

Surface charge of the obtained films and fibers containing the cationic polymers was determined following a method previously described in literature.^[28,30] Films or mat samples of 1 × 1 cm² (2 cm² surface area) were placed in 10 mL of 0.05 wt.% aqueous sodium fluorescein solution for 10 min. Then, each sample was rinsed extensively with distilled water and sonicated to remove residual fluorescein. After that, the fluorescein was desorbed from the surface of the samples by treating them with 3 mL of CTAB solution (0.1 wt.%) for 20 min under shaking at 300 rpm. Subsequently, the amount of fluorescein recovered in the supernatant was determined by UV–vis spectroscopy (Lambda 35, Perkin Elmer) in solutions prepared by adding 10% v/v of 100 mM phosphate buffer (pH 8.0). The concentration of fluorescein was calculated from the absorbance values at 501 nm with an extinction coefficient of 77 m⁻¹ cm⁻¹. The accessible cationic groups were determined assuming a relation 1:1 fluorescein: accessible cationic groups.

The surface roughness of the prepared fibers and films was analyzed by optical profilometry using a Zeta-20 optical profiler (Zeta Instruments). Water contact angle measurements were performed with deionized water on a goniometer KSV Theta (KSV Instrument, Ltd., Finland) at room temperature. Water droplets of 3 μL were placed on fiber mats or films and digital images of the water droplets were taken for contact angle determination. The contact angles were measured at least six times on different sites of the surface. Each data reported is the average of measurements ± SD (standard deviation). The morphology of electrospun fibers based on PLA and PBAT polymers was studied using a scanning electron microscope (SEM) Philips XL30 with an acceleration voltage of 25 kV. The samples were coated with gold prior to scanning.

Antimicrobial Assays: The antibacterial activity of the fibers and films was measured following the E2149-13a standard method from the American Society for Testing and Materials (ASTM)^[44] against *P. aeruginosa*, *S. aureus*, and *Methicillin-Resistant S. aureus*. First, bacterial cells were cultured on 5% sheep blood Columbia agar plates for 24 h at 37 °C and then, bacterial suspensions were prepared using the McFarland turbidity scale solution at 10⁸ colony-forming units (CFU) mL⁻¹ in saline. The suspensions were further diluted to 10⁶ CFU mL⁻¹ with PBS. Next, fibers and mats (1 × 1 cm²) were placed in sterile falcon tubes containing 9 mL of PBS and 1 mL of the tested inoculum, reaching a working suspension of ≈10⁵ CFU mL⁻¹. Control experiments were also performed in the presence of PLA fiber, PBAT fiber, and PBAT film, and in the absence of sample. These suspensions were shaken at 120 rpm for 24 h. After that, the bacterial colonies were counted by the plate counting method, and the reduction percentage was calculated in comparison with the control. The measurements were made at least in triplicate.

Cell Viability Assays: Human dermal primary fibroblasts were obtained from adult male patients and isolated as previously reported.^[45] Then, cells were cultured for 3 days in Dulbecco's modified Eagle's medium (DMEM) high glucose, supplemented with 10% fetal bovine serum (FBS), 1% penicillin/streptomycin, 1% L-glutamine, 1% Na-pyruvate, and 1% non-essential amino acids (Sigma–Aldrich, Co. Saint Louis, MO, USA) at 37 °C and 5% CO₂. To study the suitability of the obtained fiber mats and films to human fibroblast cells, cell viability tests were performed. In brief, films and fiber mats (6 mm diameter) were set down into 96-well tissue culture plates and then, cells were added into the wells at a density of 5 × 10³ cells per well and cultured for 24 h at 37 °C and 5% CO₂. As negative control, cells was seeded into a well without sample. After incubation time, the viability of cells seeded on the fibers and films mats as well as of cells growth on the wells was quantified by measuring the mitochondrial dehydrogenase activity using the dye 3-(4,5-dimethylthiazol-2-yl)-

5-(3-carboxymethoxyphenyl)2-(4-sulfophenyl)-2H-tetrazolium (MTS). The culture media was removed and fibers and films were put into a clean well. Then, 100 μL the MTS dye solution was added in each well and cells were incubated for 4 h to allow the formation of soluble formazan crystals by viable cells. Color variation was monitored as cell viability and measured at 492 nm using a microplate reader (NB-12-0035, NeBiotech, Holden, MA, USA). All the measurements were performed in triplicate.

Evaluation of Morphology of Cells Seeded onto Fibers and Films: The cell morphology of cells seeded onto fibers and films was observed by field emission scanning electron microscope (FESEM, AURIGA Zeiss). A total of 2 × 10⁴ fibroblasts were seeded onto fibers and films as described above and incubated for 24 h. At the end of this incubation, the fibers and films containing the cells were fixed in 2.5% glutaraldehyde in phosphate buffer saline for 3 h, and then, dehydrated through a graded series of ethyl alcohol. For analysis, samples were fixed onto stubs and gold sputtered and analyzed by FESEM, AURIGA Zeiss.

Supporting Information

Supporting Information is available from the Wiley Online Library or from the author.

Acknowledgements

This work was funded by the MICINN (PID2019-104600RB-I00), the Agencia Estatal de Investigación (AEI, Spain) and Fondo Europeo de Desarrollo Regional (FEDER, EU) and by CSIC (LINKA20364). A.C. acknowledges MICIU for his FPU fellowship FPU18/01776. The negativ exponents were corrected on January 16, 2023.

Conflict of Interest

The authors declare no conflict of interest.

Data Availability Statement

Research data are not shared.

Keywords

antimicrobial fibers, cell viability, cytostatic effect, electrospinning, poly(lactic) acid

Received: September 22, 2022
Revised: November 4, 2022
Published online: December 8, 2022

- [1] S. Agarwal, J. H. Wendorff, A. Greiner, *Polymer (Guildf)* **2008**, *49*, 5603.
- [2] S. Deshmukh, M. Kathiresan, M. A. Kulandainathan, *Biomater. Sci.* **2022**, *10*, 4424.
- [3] A. A. Nayl, A. I. Abd-Elhamid, N. S. Awwad, M. A. Abdelgawad, J. Wu, X. Mo, S. M. Gomha, A. A. Aly, S. Bräse, *Polymers (Basel, Switz.)* **2022**, *14*, 1508.
- [4] I. Maliszewska, T. Czapka, *Polymers (Basel, Switz.)* **2022**, *14*, 1661.
- [5] G.-M. Lanno, C. Ramos, L. Preem, M. Putrinš, I. Laidmäe, T. Tenson, K. Kogermann, *ACS Omega* **2020**, *5*, 30011.
- [6] M. Hajikhani, Z. Emam-Djomeh, G. Askari, *Int. J. Biol. Macromol.* **2021**, *172*, 143.

- [7] C. Echeverría, A. Muñoz-Bonilla, R. Cuervo-Rodríguez, D. López, M. Fernández-García, *ACS Appl. Bio Mater.* **2019**, *2*, 4714.
- [8] A. Keirouz, N. Radacsi, Q. Ren, A. Dommann, G. Beldi, K. Maniura-Weber, R. M. Rossi, G. Fortunato, *J. Nanobiotechnol.* **2020**, *18*, 51.
- [9] R. G. Shahi, M. T. P. Albuquerque, E. A. Münchow, S. B. Blanchard, R. L. Gregory, M. C. Bottino, *Odontology* **2017**, *105*, 354.
- [10] D. Kai, S. S. Liow, X. J. Loh, *Mater. Sci. Eng. C* **2015**, *45*, 659.
- [11] H. Maleki, B. Azimi, S. Ismaeilimoghadam, S. Danti, *Appl. Sci.* **2022**, *12*.
- [12] V. DeStefano, S. Khan, A. Tabada, *Eng. Regen.* **2020**, *1*, 76.
- [13] E. Jalali Dil, P. J. Carreau, B. D. Favis, *Polymer (Guildf)* **2015**, *68*, 202.
- [14] J. Chen, C. Rong, T. Lin, Y. Chen, J. Wu, J. You, H. Wang, Y. Li, *Macromolecules* **2021**, *54*, 2852.
- [15] W. A. Ribeiro Neto, A. C. C. De Paula, T. M. M. Martins, A. M. Goes, L. Averous, G. Schlatter, R. E. Suman Bretas, *Polym. Degrad. Stab.* **2015**, *120*, 61.
- [16] G. F. Santana-Melo, B. V. M. Rodrigues, E. Da Silva, R. Ricci, F. R. Marciano, T. J. Webster, L. M. R. Vasconcellos, A. O. Lobo, *Colloids Surf., B* **2017**, *155*, 544.
- [17] S. Liu, S. Qin, M. He, D. Zhou, Q. Qin, H. Wang, *Composites, Part B* **2020**, *199*, 108238.
- [18] W.-C. Jao, C.-H. Lin, J.-Y. Hsieh, Y.-H. Yeh, C.-Y. Liu, M.-C. Yang, *Polym. Adv. Technol.* **2010**, *21*, 543.
- [19] M. Persson, G. S. Lorite, S.-W. Cho, J. Tuukkanen, M. Skrifvars, *ACS Appl. Mater. Interfaces* **2013**, *5*, 6864.
- [20] D. Zhu, H. Cheng, J. Li, W. Zhang, Y. Shen, S. Chen, Z. Ge, S. Chen, *Mater. Sci. Eng. C* **2016**, *61*, 79.
- [21] A. R. Unnithan, N. A. M. Barakat, P. B. Tirupathi Pichiah, G. Gnanasekaran, R. Nirmala, Y.-S. Cha, C.-H. Jung, M. El-Newehy, H. Y. Kim, *Carbohydr. Polym.* **2012**, *90*, 1786.
- [22] N. Wattanawong, D. Aht-Ong, *Polym. Degrad. Stab.* **2021**, *183*, 109459.
- [23] C. Ergene, K. Yasuhara, E. F. Palermo, *Polym. Chem.* **2018**, *9*, 2407.
- [24] P. Pham, S. Oliver, C. Boyer, *Macromol. Chem. Phys.* **2022**, 2200226.
- [25] B. Cramariuc, R. Cramariuc, R. Scarlet, L. R. Manea, I. G. Lupu, O. Cramariuc, *J. Electrostat.* **2013**, *71*, 189.
- [26] M. M. Konai, B. Bhattacharjee, S. Ghosh, J. Haldar, *Biomacromolecules* **2018**, *19*, 1888.
- [27] A. Muñoz-Bonilla, M. Fernández-García, *Prog. Polym. Sci.* **2012**, *37*, 281.
- [28] H. Murata, R. R. Koepsel, K. Matyjaszewski, A. J. Russell, *Biomaterials* **2007**, *28*, 4870.
- [29] R. Kügler, O. Bouloussa, F. Rondelez, *Microbiology* **2005**, *151*, 1341.
- [30] S. Kliewer, S. G. Wicha, A. Bröker, T. Naundorf, T. Catmadim, E. K. Oellingrath, M. Rohnke, W. R. Streit, C. Vollstedt, H. Kipphardt, W. Maisona, *Colloids Surf., B* **2020**, *186*, 110679.
- [31] D. Navarro-Rodríguez, Y. Frere, P. Gramain, *J. Polym. Sci., Part A: Polym. Chem.* **1992**, *30*, 2587.
- [32] V. Milleret, T. Hefti, H. Hall, V. Vogel, D. Eberli, *Acta Biomater.* **2012**, *8*, 4349.
- [33] L. Sun, J. Guo, H. Chen, D. Zhang, L. Shang, B. Zhang, Y. Zhao, *Adv. Sci.* **2021**, *8*, 2100126.
- [34] W. Cui, X. Li, S. Zhou, J. Weng, *Polym. Degrad. Stab.* **2008**, *93*, 731.
- [35] M. Zhu, W. Zuo, H. Yu, W. Yang, Y. Chen, *J. Mater. Sci.* **2006**, *41*, 3793.
- [36] A. Chiloeches, R. Cuervo-Rodríguez, F. López-Fabal, M. Fernández-García, C. Echeverría, A. Muñoz-Bonilla, *Polym. Test.* **2022**, *109*, 107541.
- [37] A. Chiloeches, A. Funes, R. Cuervo-Rodríguez, F. López-Fabal, M. Fernández-García, C. Echeverría, A. Muñoz-Bonilla, *Polym. Chem.* **2021**, *12*, 3190.
- [38] I. Sovadinova, E. F. Palermo, M. Urban, P. Mpiga, G. A. Caputo, K. Kuroda, *Polymers* **2011**, *3*, 1512.
- [39] E. F. Palermo, K. Kuroda, *Appl. Microbiol. Biotechnol.* **2010**, *87*, 1605.
- [40] S. Metwally, U. Stachewicz, *Mater. Sci. Eng. C* **2019**, *104*, 109883.
- [41] M. Lopreiato, et al., *Condens. Matter* **2020**, *5*, 29.
- [42] A. Alba, G. Villaggio, G. M. L. Messina, M. Caruso, C. Federico, M. T. Cambria, G. Marletta, F. Sinatra, *Polymers* **2022**, *14*, 2643.
- [43] J. Li, W. Xu, J. Chen, D. Li, K. Zhang, T. Liu, J. Ding, X. Chen, *ACS Biomater. Sci. Eng.* **2018**, *4*, 2026.
- [44] ASTM E2149-13a **2013**.
- [45] M. Lopreiato, R. Cocchiola, S. Falcucci, M. Leopizzi, M. Cardone, V. Di Maio, U. Brocco, V. D'orazi, S. Calvieri, R. Scandurra, F. De Marco, A. Scotto D'abusco, *Photochem. Photobiol.* **2020**, *96*, 74.